Charge Density Wave in Kagome Lattice Intermetallic ScV_6Sn_6

Hasitha W. Suriya Arachchige,[1,*] William R. Meier,[2,†] Madalynn Marshall,[3] Takahiro Matsuoka,[2] Rui Xue,[1] Michael A. McGuire,[4] Raphael P. Hermann,[4] Huibo Cao,[3] and David Mandrus[1,2,4,‡]

[1]*Department of Physics and Astronomy, University of Tennessee Knoxville, Knoxville, Tennessee 37996, USA*
[2]*Materials Science and Engineering Department, University of Tennessee Knoxville, Knoxville, Tennessee 37996, USA*
[3]*Neutron Scattering Division, Oak Ridge National Laboratory, Oak Ridge, Tennessee 37831, USA*
[4]*Materials Science and Technology Division, Oak Ridge National Laboratory, Oak Ridge, Tennessee 37831, USA*

(Received 20 June 2022; accepted 14 October 2022; published 18 November 2022)

Materials hosting kagome lattices have drawn interest for the diverse magnetic and electronic states generated by geometric frustration. In the AV_3Sb_5 compounds (A = K, Rb, Cs), stacked vanadium kagome layers give rise to unusual charge density waves (CDW) and superconductivity. Here we report single-crystal growth and characterization of ScV_6Sn_6, a hexagonal $HfFe_6Ge_6$-type compound that shares this structural motif. We identify a first-order phase transition at 92 K. Single crystal x-ray and neutron diffraction reveal a charge density wave modulation of the atomic lattice below this temperature. This is a distinctly different structural mode than that observed in the AV_3Sb_5 compounds, but both modes have been anticipated in kagome metals. The diverse $HfFe_6Ge_6$ family offers more opportunities to tune ScV_6Sn_6 and explore density wave order in kagome lattice materials.

DOI: 10.1103/PhysRevLett.129.216402

Geometrically frustrated atomic arrangements hold special interest for condensed matter physics. One example, the kagome lattice, is composed of triangles and hexagons [Fig. 1(a)]. Tight binding models yield an electronic structure hosting Dirac nodes, van Hove singularities, and flat bands [Fig. 1(b)] [1,2]. Depending on band filling and interactions, a wide variety of electronic states can be realized including charge density waves (CDWs), spin density waves, bond order, and superconductivity [3–20]. A charge density wave is a redistribution of charge density in metals and an associated periodic atomic displacement that develop on cooling [21].

The hexagonal AV_3Sb_5 compounds (A = K, Rb, Cs) are a rich family of strongly correlated materials [23–26]. Stacked vanadium kagome layers in these materials give rise to CDWs and superconductivity. The origin of the CDW is closely tied to van Hove singularities at the Fermi level [27–30]. The unusual characteristics of the CDW [24,28,31–36] and its interaction with superconductivity [37–40] have sparked great interest in kagome lattice derived charge order [41].

The hexagonal $HfFe_6Ge_6$-type "166" compounds are a large family of intermetallics related to CoSn [42,43]. Unlike CoSn and AV_3Sb_5, these RM_6X_6 compounds have two kagome sheets per unit cell separated by alternating RX_2 and X_2 layers [Fig. 1(c)]. We focus on the RV_6Sn_6 compounds as they host the vanadium kagome lattice so integral to the exciting behavior in AV_3Sb_5 [44–49]. In fact, the rare earth variants even possess similar filling of the vanadium d-orbital bands [23,30,44,47]. Although the band structure and f-orbital magnetism have garnered some interest in RV_6Sn_6 (R = Y, Gd-Tm, and Lu) [44–47,49–52] no vanadium-driven order has been observed to date.

In this Letter we examine the low-temperature behavior of single crystals of the kagome metal ScV_6Sn_6. Physical property measurements reveal a first-order phase transition around 92 K reminiscent of that in the AV_3Sb_5 compounds. X-ray and neutron diffraction reveal a CDW below this temperature that is distinctly different than those in AV_3Sb_5 [26,27,29,32,35]. The CDW we identify in ScV_6Sn_6 demonstrates that charge order is a common feature in partly filled d-orbital kagome systems. Compared to the AV_3Sb_5 compounds, the $HfFe_6Ge_6$-type compounds offer improved tuneability making them an ideal platform to explore the curious CDWs in transition metal kagome systems.

Methods.—Single crystals were grown from a molten Sn flux using an atomic ratio of Sc:V:Sn = 1:6:60. Dendritic scandium metal (Alfa Aesar 99.9%), vanadium pieces (Alfa Aesar 99.8%), and Sn shot (Alfa Aesar 99.99 + %) were loaded into a 2 ml alumina Canfield crucible set [53]. The crucible assembly was sealed in an argon-filled fused silica ampule. Subsequently, the ampule was heated up to 1150 °C over 12 h followed by a 15 h dwell. Crystals were grown during a slow cool over 300 h to 780 °C. Single crystals were extracted from the melt by centrifuging.

The ScV_6Sn_6 crystals are nicely faceted metallic barrel-shaped hexagonal blocks roughly 1–3 mm in size and their $HfFe_6Ge_6$-type structure was established by powder x-ray diffraction (Supplemental Material [54]). Sn and VSn_3 were removed from crystals with 10 wt% aqueous HCl. Crystal composition was estimated using energy dispersive

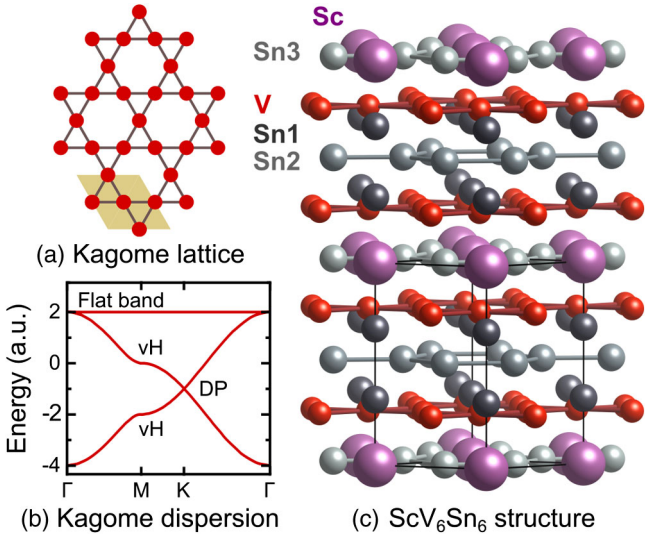

FIG. 1. (a) Kagome lattice, (b) tight-binding kagome lattice electron dispersion from Ref. [1] highlighting flat band, van Hove points (vH), and Dirac points (DP). (c) ScV_6Sn_6 structure generated with Vesta [22].

spectroscopy (EDS) on a polished surface giving $Sc:V:Sn = 1:6.21(7):6.22(11)$.

Low-temperature lattice parameters were estimated from Rietveld fits of powder x-ray diffraction (PXRD) patterns obtained using an Oxford PheniX closed-cycle helium cryostat on a PANalytical Xpert Pro diffactometer with a Cu K_α source.

Single crystal x-ray diffraction (SCXRD) studies were performed at 280 and 50 K with a Rigaku XtaLAB PRO diffractometer using Mo K_α radiation, a Rigaku HyPix-6000HE detector, and an Oxford N-HeliX cryocooler. Rigaku Oxford Diffraction CrysAlisPro [55] was used for peak indexing and integration and JANA or Shelx for structural refinement [56–59].

Single crystal neutron diffraction (SCND) was measured at HB-3A DEMAND [60] at the High Flux Isotope Reactor at Oak Ridge National Laboratory using 1.542 Å neutrons from a bent Si-220 monochromator [61]. A $2 \times 2 \times 1$ mm^3 crystal of ScV_6Sn_6 was placed inside a closed-cycle refrigerator (CCR) and the $\frac{1}{3}\frac{1}{3}\frac{10}{3}$ superlattice peak was measured on warming and cooling.

^{119}Sn Mössbauer spectra of ScV_6Sn_6 were measured at numerous temperatures on a 28 mg/cm^2 powder sample using a Janis SH-850 closed-cycle cryostat and a constant-acceleration Wissel drive. A 0.1 mCi $^{119\,m}$Sn source and a 2 in diameter Ametek Tl@NaI detector were employed with a 25 μm Pd foil between sample and detector.

Electrical resistivity measurements were obtained using four electrodes on a bar-shaped polished crystal with current perpendicular to the c axis. Resistivity was measured with a Keithley 2450 SourceMeter (sourcing current) and a 2182 Nanovoltmeter setup controlled by LabView. Temperature control and magnetic field were provided by a Quantum design physical property measurement system (PPMS) with magnetic field along c.

For magnetization measurements, an acid-etched crystal was mounted in a plastic drinking straws in a Quantum Design MPMS 3 using the vibrating sample magnetometer (VSM) option. The moment was measured between 3 and 300 K in a field of 1 T applied perpendicular to c.

Finally, heat capacity measurements were carried out using the heat capacity option of the PPMS with a 7.95 mg crystal mounted with Apiezon N grease. Data were collected between 2 and 200 K by applying a series of heat pulses that each raised the sample temperature by about 30% and analyzing the sample temperature vs time during heating and the subsequent cooling [62]. Near the transition temperature, heating and cooling curves were processed separately to observe the thermal hysteresis associated with the transition.

Results.—Figure 2 presents temperature-dependent measurements of ScV_6Sn_6 revealing a phase transition around 92 K. Magnetic susceptibility (χ_m) in Fig. 2(a) reveals a weak Pauli paramagnetic response [63,64] slightly larger than the 0.001–0.002 cm^3/mol observed for YV_6Sn_6 [44,45]. In contrast to the yttrium compound, ScV_6Sn_6 has an abrupt 20% drop in the susceptibility on cooling through 92 K.

The transition observed in magnetization is corroborated by electrical resistivity, Fig. 2(b). ScV_6Sn_6 displays metallic resistivity decreasing from 164 to 28 μΩ cm from 300 to 2 K and no bulk superconductivity down to 80 mK. Critically, there is a conspicuous 35% drop in resistivity on cooling through 92 K. The YV_6Sn_6, GdV_6Sn_6, and TbV_6Sn_6 do not have a steplike feature and have smaller resistivities across the whole temperature range [44–47].

Heat capacity provides clear evidence that the features in $\chi_m(T)$ and $\rho(T)$ correspond to a bulk phase transition in ScV_6Sn_6. Figure 2(c) presents the specific heat capacity, $C_p(T)$. A sharp peak in the heat capacity represents the heat of transformation across a first-order phase transition. This first-order nature of the transition is evident in the discontinuities in $\chi_m(T)$ and $\rho(T)$ as well as the ~0.3–1 K thermal hysteresis observed in these measurements.

The temperature dependence of the lattice parameters in Fig. 2(d) demonstrates that the phase transition in ScV_6Sn_6 couples to the crystal lattice. On cooling through the 92 K transition, c increases by 0.04% but a remains relatively unchanged.

SCXRD reveals a CDW below the 92 K phase transition in ScV_6Sn_6. Figure 3(a) presents the diffracted intensity in the HHL plane at 280 and 50 K. On cooling, new spots are observed that can be indexed by a $\frac{1}{3}\frac{1}{3}\frac{1}{3}$ propagation vector. These superlattice peaks are evidence of a commensurate CDW, a periodic displacement of the atom lattice [65]. SCND reveal that superlattice peak intensity appears near 92 K and grows on cooling [Fig. 3(b)] demonstrating the connection between the CDW and the transition evident in Fig. 2.

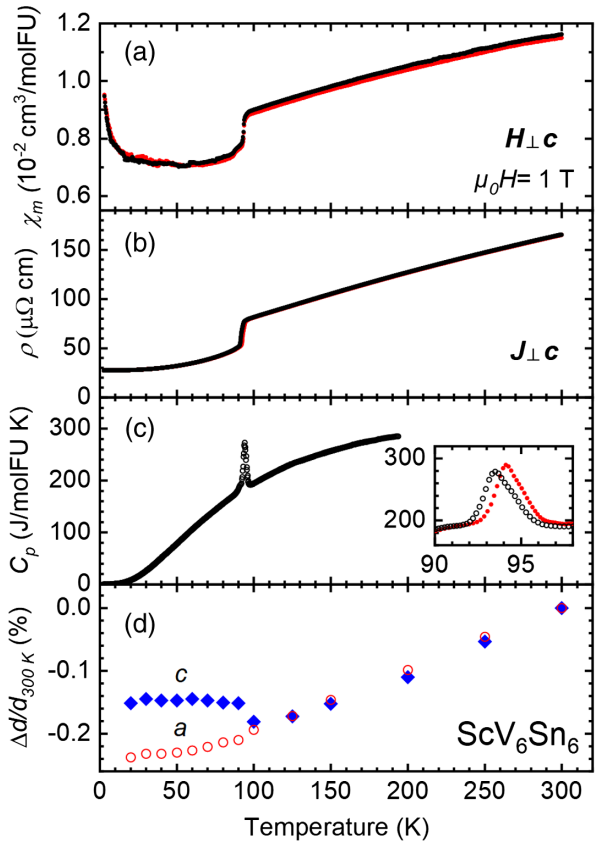

FIG. 2. Low-temperature properties of ScV_6Sn_6 reveal a first-order phase transition at 92 K. (a) Temperature dependence of magnetic susceptibility, χ_m, on cooling (black) and warming (red). (b) Temperature dependence of resistivity ρ in the ab plane measured on cooling (black) and warming (red). (c) Specific heat capacity of ScV_6Sn_6, C_p, from processing warming and cooling parts of each pulse.. The inset shows the data from the warming (red) and cooling (black) segments of each heat pulse. (d) Relative change in ScV_6Sn_6 lattice parameters vs temperature.

The refined $R32$ low temperature structure is presented in Supplemental Material [54] and is dominated by the displacement mode transforming as the irreducible representation P_1 of $P6/mmm$ (notation from ISODISTORT and Amplimodes applications) [66–69].

Mössbauer spectroscopy reveals that the Sn atoms see this structural modulation Fig. 3(c). On cooling through the 92 K transition the absorption spectra abruptly change shape as reflected by a step of the average quadrupole splitting (Fig. 3(c) and the Supplemental Material [54]).

Discussion.—The CDW in ScV_6Sn_6 has similarities to the CDWs in the AV_3Sb_5 compounds. First, both compounds host vanadium kagome lattices with V-V distances between 2.73 and 2.75 Å [23]. The Fermi level sits within vanadium d-orbital bands in both the AV_3Sb_5 compounds [23,26,28,29,41,70] and GdV_6Sn_6 [44,45,49,50]. It is likely that the vanadium bands play a key role in CDW formation in ScV_6Sn_6 as they do in the AV_3Sb_5 compounds [26,28–30].

Second, the CDWs have a similar impact on the physical properties in these materials. For example, the CDW in CsV_3Sb_5 is accompanied by a sharp drop of both magnetic susceptibility and in-plane resistivity on cooling [26,32,34] just as we observe in Fig. 2. Discontinuities in resistance and magnetic susceptibility are frequent signatures of CDW modifications of the electronic structure [65,71–73].

Importantly, the CDWs in AV_3Sb_5 family and ScV_6Sn_6 have two important differences. First, the modulation wave vectors in the two compounds are different. We observe a $\frac{1}{3}\frac{1}{3}\frac{1}{3}$ wave vector in ScV_6Sn_6 tripling the ab-plane area of the cell [Fig. 3(e)]. Along c, the rhombohedral structure repeats every three unit cells [Fig. 3(f) and the Supplemental Material [54]]. In contrast, the $\frac{1}{2}\frac{1}{2}\frac{1}{2}$ or $\frac{1}{2}\frac{1}{2}\frac{1}{4}$ CDW in the AV_3Sb_5 compounds quadruples the unit cell in the ab plane [Figs. 3(g) and 3(h)] and doubles or quadruples the c axis [26,27,29,31–33,41,74].

The second key difference between the CDWs in these compounds is the displacements of the vanadium atoms. In CsV_3Sb_5, the vanadium atoms displace in the plane by 0.009–0.085 Å forming either the Star of David or tri-hexagonal arrangement [Figs. 3(g) and 3(h)] [29]. In contrast, our refinement suggests that Sc and Sn1 have the largest modulated displacements in ScV_6Sn_6. We estimate Sc and Sn1 displace up to 0.16 Å along the c axis. The vanadium atoms appear to have a far weaker response, displacing only 0.004–0.006 Å.

CDWs and bond density waves are prominent instabilities of partly filled kagome bands. Charge order is favored by nearest neighbor Coulomb repulsion for $\frac{1}{3}$ and $\frac{2}{3}$ filled kagome bands [4,8–11,18,20]. In fact, the $\frac{1}{2}\frac{1}{2}$ and $\frac{1}{3}\frac{1}{3}$ in-plane modulation of the kagome sheet are favored by nearest neighbor Coulomb repulsion [4,9–11]. The weak vanadium displacements we infer from our ScV_6Sn_6 diffraction data could be due to some of the exotic orders proposed in the kagome lattice involving chiral currents and bond orders [6,11,12,15,16,20,31,35]. One of the exciting questions about the CDW in AV_3Sb_5 is whether or not it breaks time reversal symmetry [34,36,75–82]. Does the CDW in ScV_6Sn_6 have time reversal symmetry breaking or chiral character?

Upcoming investigations of the CDW in ScV_6Sn_6 have a distinct advantage over the AV_3Sb_5 compounds: tuneability. Although KV_3Sb_5, RbV_3Sb_5, and CsV_3Sb_5 compounds have generated significant excitement, the family is quite small [23] (despite proposed variants [83]). Doping opportunities are also limited to Ti or Nb for V [84,85] and Sn for Sb [40,86]. In contrast, the RM_6X_6 compounds of the $HfFe_6Ge_6$ family are far more diverse [42] offering many different options for tuning the CDW in ScV_6Sn_6 to uncover what factors influence charge order and superconductivity in kagome metals. To start, it is curious that only the Sc variant of the RV_6Sn_6 compounds display a CDW so far [44–47,51].

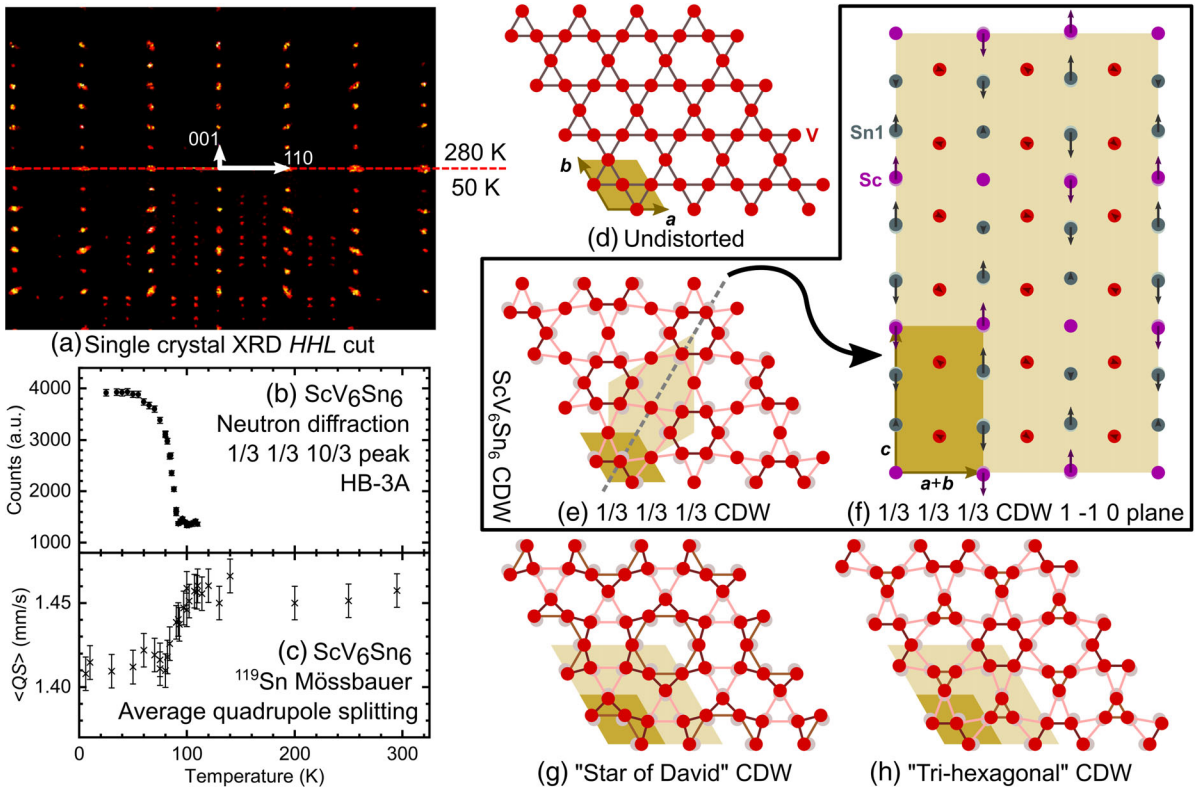

FIG. 3. Details of the CDW in ScV_6Sn_6 (a) single crystal diffraction intensity in the HHL plane. New peaks at 50 K signal a structural modulation with wave-vector $\frac{1}{3}\frac{1}{3}\frac{1}{3}$. (b) Single crystal neutron diffraction intensity from the $\frac{1}{3}\frac{1}{3}\frac{10}{3}$ peak. (c) Average quadrupole splitting for a three site fit to ^{119}Sn Mössbauer spectra. (d) Kagome lattice with ScV_6Sn_6 unit cell (dark yellow). (e) exaggerated P_1 $\frac{1}{3}\frac{1}{3}\frac{1}{3}$ CDW mode showing 3 times larger in-plane unit cell (light yellow). Shorter and longer bonds are darker and lighter, respectively. (f) Depiction of refined atomic displacements in $\frac{1}{3}\frac{1}{3}\frac{1}{3}$ CDW mode in a (1 -1 0) plane of ScV_6Sn_6. (g) and (h) The Star of David and trihexagonal CDW modulations of the vanadium kagome lattice in CsV_3Sb_5. These $\frac{1}{2}\frac{1}{2}\frac{1}{2}$ or $\frac{1}{2}\frac{1}{2}\frac{1}{4}$ modes quadruple the unit cell in the ab-plane (light yellow rhombi).

Conclusion.—The intriguing charge density waves (CDWs) in the AV_3Sb_5 compounds inspired us to investigate ScV_6Sn_6. Low-temperature physical property measurements reveal a first-order 92 K transition. X-ray and neutron diffraction reveal a CDW modulation of the atomic lattice below this temperature. Despite the similarities between ScV_6Sn_6 and the AV_3Sb_5 compounds, their CDWs have different propagation vectors. Excitingly, ScV_6Sn_6 belongs to a large family of compounds offering more tuning opportunities to explore the origin of charge order in kagome lattice compounds.

We thank I. I. Mazin for his discussions regarding charge density waves. M. A. M., R. P. H., and D. M. acknowledge support from the US Department of Energy, Office of Science, Basic Energy Sciences, Materials Science and Engineering Division. H. W. S. A., W. R. M., T. M., and R. X. acknowledge support from the Gordon and Betty Moore Foundation's EPiQS Initiative, Grant No. GBMF9069. M. M. and H. C. acknowledge support from the US Department of Energy (DOE), Office of Science, Office of Basic Energy Sciences, Early Career Research Program Award No. KC0402020, under Contract No. DE-AC05-00OR22725. This research used resources at the High Flux Isotope Reactor and the Spallation Neutron Source, the DOE Office of Science User Facility operated by ORNL. Powder XRD was performed at the Institute for Advanced Materials & Manufacturing (IAMM) Diffraction Facility with the assistance of Michael R. Koehler, located at the University of Tennessee, Knoxville. This manuscript has been authored by UT-Battelle, LLC under Contract No. DE-AC05-00OR22725 with the U.S. Department of Energy. The United States Government retains and the publisher, by accepting the article for publication, acknowledges that the United States Government retains a non-exclusive, paid-up, irrevocable, worldwide license to publish or reproduce the published form of this manuscript, or allow others to do so, for United States Government purposes. The Department of Energy will provide public access to these results of federally sponsored research in accordance with the DOE Public Access Plan [87].

*ssuriyaa@vols.utk.edu
†javamocham@gmail.com
‡dmandrus@utk.edu

[1] W. Beugeling, J. C. Everts, and C. M. Smith, Phys. Rev. B **86**, 195129 (2012).
[2] H.-M. Guo and M. Franz, Phys. Rev. B **80**, 113102 (2009).
[3] M. H. Christensen, T. Birol, B. M. Andersen, and R. M. Fernandes, Phys. Rev. B **104**, 214513 (2021).
[4] W.-S. Wang, Z.-Z. Li, Y.-Y. Xiang, and Q.-H. Wang, Phys. Rev. B **87**, 115135 (2013).
[5] H. Tan, Y. Liu, Z. Wang, and B. Yan, Phys. Rev. Lett. **127**, 046401 (2021).
[6] X. Feng, K. Jiang, Z. Wang, and J. Hu, Sci. Bull. **66**, 1384 (2021).
[7] S. V. Isakov, S. Wessel, R. G. Melko, K. Sengupta, and Y. B. Kim, Phys. Rev. Lett. **97**, 147202 (2006).
[8] A. O'Brien, F. Pollmann, and P. Fulde, Phys. Rev. B **81**, 235115 (2010).
[9] A. Rüegg and G. A. Fiete, Phys. Rev. B **83**, 165118 (2011).
[10] J. Wen, A. Rüegg, C.-C. J. Wang, and G. A. Fiete, Phys. Rev. B **82**, 075125 (2010).
[11] S. Nishimoto, M. Nakamura, A. O'Brien, and P. Fulde, Phys. Rev. Lett. **104**, 196401 (2010).
[12] M. L. Kiesel, C. Platt, and R. Thomale, Phys. Rev. Lett. **110**, 126405 (2013).
[13] K. Barros, J. W. F. Venderbos, G.-W. Chern, and C. D. Batista, Phys. Rev. B **90**, 245119 (2014).
[14] S.-L. Yu and J.-X. Li, Phys. Rev. B **85**, 144402 (2012).
[15] M. M. Denner, R. Thomale, and T. Neupert, Phys. Rev. Lett. **127**, 217601 (2021).
[16] X. Feng, Y. Zhang, K. Jiang, and J. Hu, Phys. Rev. B **104**, 165136 (2021).
[17] M. L. Kiesel and R. Thomale, Phys. Rev. B **86**, 121105(R) (2012).
[18] F. Ferrari, F. Becca, and R. Valentí, Phys. Rev. B **106**, L081107 (2022).
[19] W.-H. Ko, P. A. Lee, and X.-G. Wen, Phys. Rev. B **79**, 214502 (2009).
[20] T. Park, M. Ye, and L. Balents, Phys. Rev. B **104**, 035142 (2021).
[21] X. Zhu, J. Guo, J. Zhang, and E. W. Plummer, Adv. Phys. X **2**, 622 (2017).
[22] K. Momma and F. Izumi, J. Appl. Crystallogr. **44**, 1272 (2011).
[23] B. R. Ortiz, L. C. Gomes, J. R. Morey, M. Winiarski, M. Bordelon, J. S. Mangum, I. W. H. Oswald, J. A. Rodriguez-Rivera, J. R. Neilson, S. D. Wilson, E. Ertekin, T. M. McQueen, and E. S. Toberer, Phys. Rev. Mater. **3**, 094407 (2019).
[24] B. R. Ortiz, P. M. Sarte, E. M. Kenney, M. J. Graf, S. M. L. Teicher, R. Seshadri, and S. D. Wilson, Phys. Rev. Mater. **5**, 034801 (2021).
[25] Q. Yin, Z. Tu, C. Gong, Y. Fu, S. Yan, and H. Lei, Chin. Phys. Lett. **38**, 037403 (2021).
[26] B. R. Ortiz, S. M. L. Teicher, Y. Hu, J. L. Zuo, P. M. Sarte, E. C. Schueller, A. M. M. Abeykoon, M. J. Krogstad, S. Rosenkranz, R. Osborn, R. Seshadri, L. Balents, J. He, and S. D. Wilson, Phys. Rev. Lett. **125**, 247002 (2020).
[27] Z. Liang, X. Hou, F. Zhang, W. Ma, P. Wu, Z. Zhang, F. Yu, J.-J. Ying, K. Jiang, L. Shan, Z. Wang, and X.-H. Chen, Phys. Rev. X **11**, 031026 (2021).
[28] M. Kang, S. Fang, J.-K. Kim, B. R. Ortiz, S. H. Ryu, J. Kim, J. Yoo, G. Sangiovanni, D. D. Sante, B.-G. Park, C. Jozwiak, A. Bostwick, E. Rotenberg, E. Kaxiras, S. D. Wilson, J.-H. Park, and R. Comin, Nat. Phys. **18**, 301 (2022).
[29] B. R. Ortiz, S. M. L. Teicher, L. Kautzsch, P. M. Sarte, N. Ratcliff, J. Harter, J. P. C. Ruff, R. Seshadri, and S. D. Wilson, Phys. Rev. X **11**, 041030 (2021).
[30] Y. Hu, X. Wu, B. R. Ortiz, S. Ju, X. Han, J. Ma, N. C. Plumb, M. Radovic, R. Thomale, S. D. Wilson, A. P. Schnyder, and M. Shi, Nat. Commun. **13**, 2220 (2022).
[31] L. Nie, K. Sun, W. Ma, D. Song, L. Zheng, Z. Liang, P. Wu, F. Yu, J. Li, M. Shan, D. Zhao, S. Li, B. Kang, Z. Wu, Y. Zhou, K. Liu, Z. Xiang, J. Ying, Z. Wang, T. Wu, and X. Chen, Nature (London) **604**, 59 (2022).
[32] Z. Wang *et al.*, Phys. Rev. B **104**, 075148 (2021).
[33] H. Li, T. T. Zhang, T. Yilmaz, Y. Y. Pai, C. E. Marvinney, A. Said, Q. W. Yin, C. S. Gong, Z. J. Tu, E. Vescovo, C. S. Nelson, R. G. Moore, S. Murakami, H. C. Lei, H. N. Lee, B. J. Lawrie, and H. Miao, Phys. Rev. X **11**, 031050 (2021).
[34] F. H. Yu, T. Wu, Z. Y. Wang, B. Lei, W. Z. Zhuo, J. J. Ying, and X. H. Chen, Phys. Rev. B **104**, L041103 (2021).
[35] Y.-X. Jiang *et al.*, Nat. Mater. **20**, 1353 (2021).
[36] S.-Y. Yang, Y. Wang, B. R. Ortiz, D. Liu, J. Gayles, E. Derunova, R. Gonzalez-Hernandez, L. Šmejkal, Y. Chen, S. S. P. Parkin, S. D. Wilson, E. S. Toberer, T. McQueen, and M. N. Ali, Sci. Adv. **6**, eabb6003 (2020).
[37] F. H. Yu, D. H. Ma, W. Z. Zhuo, S. Q. Liu, X. K. Wen, B. Lei, J. J. Ying, and X. H. Chen, Nat. Commun. **12**, 3645 (2021).
[38] H. Chen *et al.*, Nature (London) **599**, 222 (2021).
[39] F. Du, S. Luo, B. R. Ortiz, Y. Chen, W. Duan, D. Zhang, X. Lu, S. D. Wilson, Y. Song, and H. Yuan, Phys. Rev. B **103**, L220504 (2021).
[40] Y. M. Oey, B. R. Ortiz, F. Kaboudvand, J. Frassineti, E. Garcia, R. Cong, S. Sanna, V. F. Mitrović, R. Seshadri, and S. D. Wilson, Phys. Rev. Mater. **6**, L041801 (2022).
[41] T. Neupert, M. M. Denner, J.-X. Yin, R. Thomale, and M. Z. Hasan, Nat. Phys. **18**, 137 (2022).
[42] G. Venturini, Z. Kristallogr. -Cryst. Mater. **221**, 511 (2006).
[43] N. J. Ghimire, R. L. Dally, L. Poudel, D. Jones, D. Michel, N. T. Magar, M. Bleuel, M. A. McGuire, J. Jiang, J. Mitchell, and I. Mazin, Sci. Adv. **6**, eabe2680 (2020).
[44] G. Pokharel, S. M. L. Teicher, B. R. Ortiz, P. M. Sarte, G. Wu, S. Peng, J. He, R. Seshadri, and S. D. Wilson, Phys. Rev. B **104**, 235139 (2021).
[45] H. Ishikawa, T. Yajima, M. Kawamura, H. Mitamura, and K. Kindo, J. Phys. Soc. Jpn. **90**, 124704 (2021).
[46] G. Pokharel, B. Ortiz, P. Sarte, L. Kautzsch, G. Wu, J. Ruff, and S. D. Wilson, arXiv:2205.15559.
[47] E. Rosenberg, J. M. DeStefano, Y. Guo, J. S. Oh, M. Hashimoto, D. Lu, R. J. Birgeneau, Y. Lee, L. Ke, M. Yi, and J.-H. Chu, Phys. Rev. B **106**, 115139 (2022).
[48] L. Romaka, M. Konyk, Y. Stadnyk, V. V. Romaka, and R. Serkiz, Phys. Chem. Solid State **20**, 69 (2019).

[49] S. Peng, Y. Han, G. Pokharel, J. Shen, Z. Li, M. Hashimoto, D. Lu, B. R. Ortiz, Y. Luo, H. Li, M. Guo, B. Wang, S. Cui, Z. Sun, Z. Qiao, S. D. Wilson, and J. He, Phys. Rev. Lett. **127**, 266401 (2021).

[50] Y. Hu, X. Wu, Y. Yang, S. Gao, N. C. Plumb, A. P. Schnyder, W. Xie, J. Ma, and M. Shi, Sci. Adv. **8**, eadd2024 (2022).

[51] J. Lee and E. Mun, arXiv:2206.02924.

[52] X. X. Zhang, Z. Y. Liu, Q. Cui, N. N. Wang, L. F. Shi, H. Zhang, X. L. Dong, J. P. Sun, Z. L. Dun, and J. G. Cheng, arXiv:2206.05653.

[53] P. C. Canfield, T. Kong, U. S. Kaluarachchi, and N. H. Jo, Philos. Mag. **96**, 84 (2016).

[54] See Supplemental Material at http://link.aps.org/supplemental/10.1103/PhysRevLett.129.216402 for details of the refined crystal structure of ScV_6Sn_6, a photo of a crystal and detailed discussion of the Mössbauer experiment. The refined high and low temperature ScV_6Sn_6 crystal structure .cif files are also included.

[55] *CrysAlisPRO*, Oxford Diffraction/Agilent Technologies UK Ltd, Yarnton, England.

[56] V. Petříček, M. Dušek, and L. Palatinus, Z. Kristallogr.-Cryst. Mater. **229**, 345 (2014).

[57] P. J. Becker and P. Coppens, Acta Crystallogr. Sect. A **30**, 129 (1974).

[58] G. M. Sheldrick, Acta Crystallogr. Sect. C **71**, 3 (2015).

[59] G. M. Sheldrick, Acta Crystallogr. Sect. A **71**, 3 (2015).

[60] H. Cao, B. Chakoumakos, K. Andrews, Y. Wu, R. Riedel, J. Hodges, W. Zhou, R. Gregory, B. Haberl, J. Molaison, and G. Lynn, Crystals **9**, 5 (2018).

[61] B. C. Chakoumakos, H. Cao, F. Ye, A. D. Stoica, M. Popovici, M. Sundaram, W. Zhou, J. S. Hicks, G. W. Lynn, and R. A. Riedel, J. Appl. Crystallogr. **44**, 655 (2011).

[62] *Quantum Design Physical Property Measurement System Heat Capacity Option User's Manual*, 11th ed. (Quantum Design, San Diego, 2004), https://www.mrl.ucsb.edu/sites/default/files/mrl_docs/instruments/hcapPPMS.pdf.

[63] S. Blundell, *Magnetism in Condensed Matter* (Oxford University Press, USA, 2001).

[64] C. Kittel, *Introduction to Solid State Physics*, 8th ed. (John Wiley & Sons Inc, Hoboken, NJ, 2004).

[65] G. Grüner, *Density Waves in Solids* (Perseus Publishing, Cambridge, Mass., 1994).

[66] B. J. Campbell, H. T. Stokes, D. E. Tanner, and D. M. Hatch, J. Appl. Crystallogr. **39**, 607 (2006).

[67] H. T. Stokes, D. M. Hatch, and B. J. Campbell, ISODISTORT, ISOTROPY software suite, version 6.7.2, 2020.

[68] D. Orobengoa, C. Capillas, M. I. Aroyo, and J. M. Perez-Mato, J. Appl. Crystallogr. **42**, 820 (2009).

[69] J. M. Perez-Mato, D. Orobengoa, and M. I. Aroyo, Acta Crystallogr. Sect. A **66**, 558 (2010).

[70] H. LaBollita and A. S. Botana, Phys. Rev. B **104**, 205129 (2021).

[71] W. R. Meier, B. C. Chakoumakos, S. Okamoto, M. A. McGuire, R. P. Hermann, G. D. Samolyuk, S. Gao, Q. Zhang, M. B. Stone, A. D. Christianson, and B. C. Sales, Chem. Mater. **33**, 2855 (2021).

[72] S. Ramakrishnan, A. Schönleber, T. Rekis, N. van Well, L. Noohinejad, S. van Smaalen, M. Tolkiehn, C. Paulmann, B. Bag, A. Thamizhavel, D. Pal, and S. Ramakrishnan, Phys. Rev. B **101**, 060101(R) (2020).

[73] Y. Singh, D. Pal, S. Ramakrishnan, A. M. Awasthi, and S. K. Malik, Phys. Rev. B **71**, 045109 (2005).

[74] C. Mu, Q. Yin, Z. Tu, C. Gong, H. Lei, Z. Li, and J. Luo, Chin. Phys. Lett. **38**, 077402 (2021).

[75] X. Zhou, H. Liu, W. Wu, K. Jiang, Y. Shi, Z. Li, Y. Sui, J. Hu, and J. Luo, Phys. Rev. B **105**, 205104 (2022).

[76] C. Mielke *et al.*, Nature (London) **602**, 245 (2022).

[77] L. Yu, C. Wang, Y. Zhang, M. Sander, S. Ni, Z. Lu, S. Ma, Z. Wang, Z. Zhao, H. Chen, K. Jiang, Y. Zhang, H. Yang, F. Zhou, X. Dong, S. L. Johnson, M. J. Graf, J. Hu, H.-J. Gao, and Z. Zhao, arXiv:2107.10714.

[78] R. Khasanov, D. Das, R. Gupta, C. Mielke, M. Elender, Q. Yin, Z. Tu, C. Gong, H. Lei, E. T. Ritz, R. M. Fernandes, T. Birol, Z. Guguchia, and H. Luetkens, Phys. Rev. Res. **4**, 023244 (2022).

[79] Q. Wu, Z. X. Wang, Q. M. Liu, R. S. Li, S. X. Xu, Q. W. Yin, C. S. Gong, Z. J. Tu, H. C. Lei, T. Dong, and N. L. Wang, arXiv:2110.11306.

[80] Y. Xu, Z. Ni, Y. Liu, B. R. Ortiz, S. D. Wilson, B. Yan, L. Balents, and L. Wu, arXiv:2204.10116.

[81] Y. Hu, S. Yamane, G. Mattoni, K. Yada, K. Obata, Y. Li, Y. Yao, Z. Wang, J. Wang, C. Farhang, J. Xia, Y. Maeno, and S. Yonezawa, arXiv:2208.08036.

[82] D. R. Saykin, C. Farhang, E. D. Kountz, D. Chen, B. R. Ortiz, C. Shekhar, C. Felser, S. D. Wilson, R. Thomale, J. Xia, and A. Kapitulnik, arXiv:2209.10570.

[83] Y. Jiang, Z. Yu, Y. Wang, T. Lu, S. Meng, K. Jiang, and M. Liu, Chin. Phys. Lett. **39**, 047402 (2022).

[84] Y. Liu, Y. Wang, Y. Cai, Z. Hao, X.-M. Ma, L. Wang, C. Liu, J. Chen, L. Zhou, J. Wang, S. Wang, H. He, Y. Liu, S. Cui, J. Wang, B. Huang, C. Chen, and J.-W. Mei, arXiv:2110.12651.

[85] T. Kato, Y. Li, K. Nakayama, Z. Wang, S. Souma, F. Matsui, M. Kitamura, K. Horiba, H. Kumigashira, T. Takahashi, Y. Yao, and T. Sato, Phys. Rev. Lett. **129**, 206402 (2022).

[86] Y. M. Oey, F. Kaboudvand, B. R. Ortiz, R. Seshadri, and S. D. Wilson, Phys. Rev. Mater. **6**, 074802 (2022).

[87] http://energy.gov/downloads/doe-public-access-plan.